Received: 20 July 2021
DOI: 10.1002/mop.33114

WILEY

RESEARCH ARTICLE

Self-sustainable wireless sensor network for low-temperature application

Young Seek Cho[1] | **Kyungjoon Choi**[2] | **Jaerock Kwon**[3]

[1]Department of Electronic Engineering, Wonkwang University, Iksan, Jeollabuk-do, Republic of Korea

[2]Department of Information and Communication Engineering, Wonkwang University, Iksan, Jeollabuk-do, Republic of Korea

[3]Department of Electrical and Computer Engineering, University of Michigan-Dearborn, Dearborn, Michigan, USA

Correspondence
Young Seek Cho, Department of Electronic Engineering, Wonkwang University, Iksan, Jeollabuk-do 54538, Republic of Korea.
Email: ycho@wku.ac.kr

Funding information
Wonkwang University

Abstract

While environmental monitoring system is an exemplary application for wireless sensor network (WSN), its energy-constraint still remains unresolved issue and needs to be addressed. In this work, a self-sustainable WSN is proposed for low-temperature application. To resolve the energy-constraint issue, a wireless power transfer (WPT) technique, called conformal strongly coupled magnetic resonant (CSCMR) technique, is adopted. At 90 MHz, the RF power transmission efficiency is 84% with 60 mm distance between transmitting and receiving resonators. For the 90 MHz RF power, the rectifier efficiency for the RF to DC power conversion is 69% and 76 at 25°C and −20°C, respectively. For an energy storage unit, a supercapacitor is chosen for the low-temperature application. With the excellent temperature characteristic of the supercapacitor, the effectiveness of the supercapacitor is verified as the energy storage unit operating at −20°C. It is shown that the WSN proposed in this work can operate in perpetuity as long as the circuit components in the WSN do not have any defects.

KEYWORDS

energy harvester, low temperature, supercapacitor, wireless sensor network (WSN)

1 | INTRODUCTION

Wireless sensor network (WSN) plays a key role in internet of things (IoT).[1] It is most desirable that the WSN works autonomously without any interruption or downtime for battery replacement or being out of power. It has been pointed out that one of the unique challenges of IoT systems[2] is the energy constraint that would limit the service time of the IoT devices. To address this energy constraint for WSNs, energy harvesting techniques was surveyed.[3] Among the energy sources such as solar, wind, vibrations, or RF energy, the RF energy is considered as a reliable energy source because the RF energy can be generated and be controllable by human as opposed to the sources from nature.

When the resonant inductive coupling scheme was introduced by Kurs et al in 2007,[4] WPT in mid-range (0.5–5 m) is in great interest.[5,6] To make Kurs's work more feasible, Hu et al developed a conformal strongly coupled magnetic resonant (CSCMR) technique.[7]

The motivation of this work is a temperature and pressure monitoring system that is essential part in industrial freeze dryers.[8] It is crucial for the temperature and pressure monitoring system to operate autonomously in a freeze dryer without interruption. A conventional way to measure temperature inside the freeze dryer is using thermocouples. The drawbacks of using thermocouples[9] demand new techniques. Some WSNs in a freeze dryer[10,11] were powered by a lithium coin cell or alkaline battery. The low-temperature in a freeze dryer is much below 0. In general, however, electrochemical batteries such as lithium-ion batteries or lithium coin cells have poor performance at low temperature.[12–14]

In this work, we design and implement a self-sustainable WSN for low-temperature application. For the implementation of the whole WSN powered by WPT with an RF energy harvester and supercapacitor, the WPT is implemented with the CSCMR technique and the WSN adopts the Zigbee protocol. The charging and discharging characteristics of a supercapacitor in −20 and 25°C are measured and analyzed to verify the effectiveness of the temperature performance of the supercapacitor. This WSN can operate autonomously in perpetuity even in a low temperature chamber.

2 | DESIGN CONSIDERATIONS FOR THE ENTIRE SYSTEM

The schematic of the wireless sensor node powered by a WPT technique with an RF energy harvester for low-temperature

application is shown in Figure 1. For the design and implementation of the entire system, several design considerations are presented in the following subsections.

2.1 | Conformal strongly coupled magnetic resonator

As mentioned in Section 1, the WPT technique is realized by the CSCMR technique. Since the WSN proposed in this work needs to be working in a restricted area such as a freeze dryer, the resonators in the CSCMR technique must be small. To reduce the size of the transmitting and receiving resonators, the operating frequency is selected to be 90 MHz. Although the operating frequency of 90 MHz is in the middle of FM radio band, 88–108 MHz, it works only in the near field zone. Thus, its operation cannot interfere the operation of FM radio broadcasting.

To design the CSCMR scheme around 90 MHz, a commercial 3D electromagnetic simulator, HFSS* was used. Basically, the resonator is an LC resonator and its resonant frequency is governed by Equation (1).

$$f_r = \frac{1}{2\pi\sqrt{LC}} \tag{1}$$

The capacitance is chosen to be 33 pF. By using the Eigenmode solver in HFSS, the dimensions of the source loop and resonator were determined to be operating around 90 MHz. The radii of the source and resonator are 16 and 28 mm, respectively. The width of the conductor for the source and resonator is the same as 6 mm. The source (or load) loop and transmitting (or receiving) resonator are on each side of a 1.5 mm thick FR4 ($\varepsilon_r = 4.5$ and $\tan\delta = 0.01$) substrate with 35 μm thick of copper.

With the dimensions of the resonator, the 3D model of the CSCMR technique, as shown in Figure 1, is simulated in HFSS. The optimum distance between the transmitting and receiving resonators is determined for the most efficient transmission performance. From the simulated and measured *S*-parameters, the efficiency (η_{WPT}) of the CSCMR technique for the RF power transmission can be calculated by the Equation (2).[7] The results will be shown in Section 3.

$$\eta_{WPT} = \frac{P_{load}}{P_{source}} = |S_{21}|^2 \tag{2}$$

2.2 | Circuit design of RF power rectifier and energy harvester

The schematics of the rectifier and energy harvester are shown in Figure 2A,B, respectively. The rectifier is realized using the conventional bridge rectifier circuit with 4 Schottky diodes. The rectifier efficiency ($\eta_{RF\text{-}DC}$) for the RF to DC power conversion can be calculated using Equation (3).[15]

$$\eta_{RF\text{-}DC} = \frac{I_{out}^2 R_L}{\left(\frac{v_{peak}}{\sqrt{2}R_s}\right)^2} \times 100 \tag{3}$$

In Equation (3), v_{peak}, R_s, I_{out}, and R_L are the peak input voltage, the output resistance of 50 Ω of an RF power generator, the output current from the rectifier, and load resistance of 887 kΩ, as shown in Figure 2A, respectively. Because the input resistance of the energy harvester, BQ25570 manufactured by Texas Instruments (TI), is 20 Ω, the load resistance of the rectifier must be very high. Thus, the load resistance of 887 kΩ is chosen in this work.

Since the current extracted from the rectifier turns out to be quite small, the rectifier itself cannot supply enough to power for a single wireless sensor node. Therefore, the rectifier is followed by the energy harvester with a rechargeable energy storage unit as shown in Figure 2B. The BQ25570 is

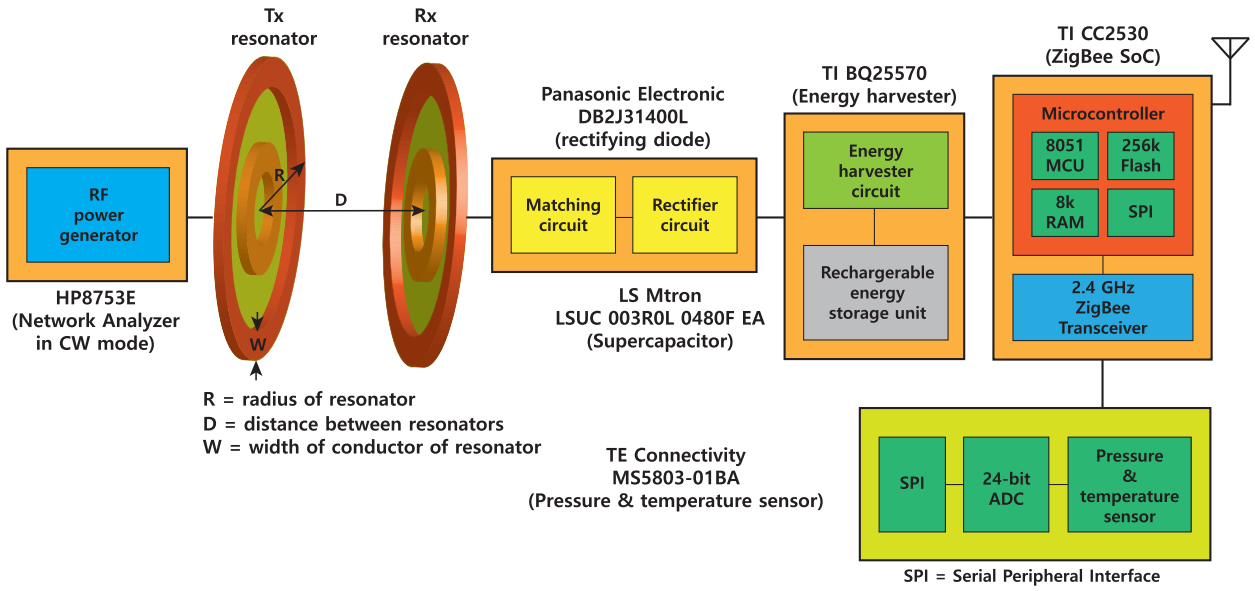

FIGURE 1 Block diagram of the wireless sensor node powered by the wireless power transfer technique with energy harvester

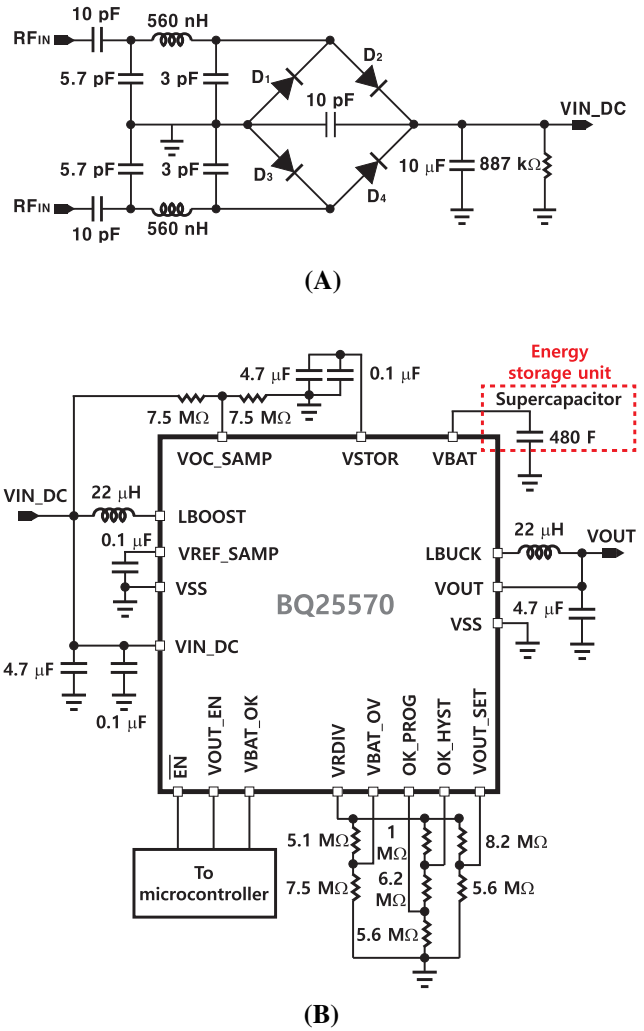

FIGURE 2 Schematics of the (A) rectifier and (B) energy harvester with an energy storage unit, a supercapacitor in this work

capable of extracting µW to mW of power from high output impedance DC sources to charge electrochemical batteries or supercapacitors. As the WSN proposed in this work is for low-temperature application, a supercapacitor is chosen.

2.3 | Wireless sensor network

Among wireless communication protocols such as Zigbee, Wi-Fi, or Bluetooth, Zigbee is adopted to implement the WSN. Zigbee is an excellent solution for WSN, as it enables to realize a stand-alone mesh network with low cost and low power consumption. The Zigbee SoC and digital multisensor are manufactured by TI and TE Connectivity, respectively. The digital multisensor can measure pressure and temperature. The pressure and temperature ranges are from 10 to 1300 mbar and from −40 to 85°C, respectively.

Two separate software modules for a transmitter and receiver were implemented. The transmitter and the receiver were implemented in the Application layer on top of TI's layered software architecture.[16] The Basic RF is a protocol layer to transmit and receive data packets through a two-way

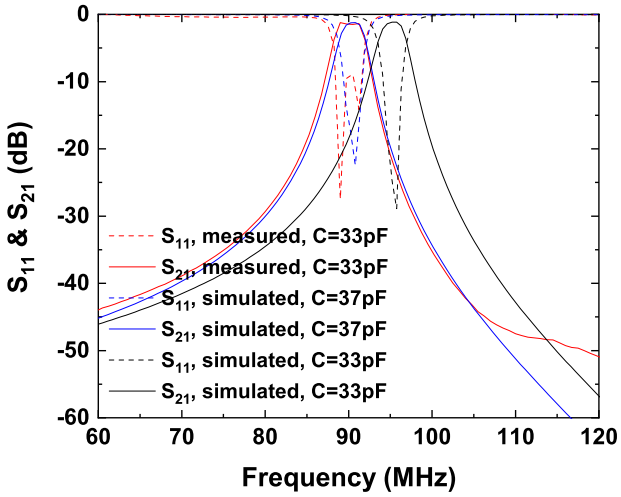

FIGURE 3 Comparison of *S*-parameters between simulated and measured results of the conformal strongly coupled magnetic resonant system

RF link. In the transmitter, a serial peripheral interface (SPI), as shown in Figure 1, was implemented with the hardware abstraction layer to communicate with the sensor modules. The transmitter's main control module, an SPI master, sends the analog/digital conversion command to the sensor module when it needs sensor readings. Then, the sensor module, an SPI slave, sends back the current sensor readings to the master.

In the receiver, an interrupt service routine (ISR) in the Basic RF is responsible for getting data from the transmitter. When a complete packet is successfully received through the ISR, the Basic RF sets a ready flag. The receiver module in the Application layer can notice that an RF packet is ready by checking the flag in a loop. When the flag is set, the receiver module will read the transmitted data. More details for the packet transmission and reception sequences can be found in TI's document.[16]

3 | RESULTS AND DISCUSSIONS

3.1 | Conformal strongly coupled magnetic resonator

The performance of the CSCMR technique is measured by HP8753E vector network analyzer. The comparison of the *S*-parameters between simulated and measured results is shown in Figure 3. As can be seen, the *S*-parameters simulated with 33 pF is off to the right compared to the measured *S*-parameters. The reason for this is because the commercial chip capacitor has some manufacturing tolerance in the capacitance. When simulated with a capacitance of 34.5 pF, as shown in Figure 3, the simulated *S*-parameters is matched very well to the measured *S*-parameters. The measured insertion loss ($|S_{21}|$) between the transmitting and receiving resonators with 60 mm distance is 1.49 dB, which results in the

η_{WPT} of the CSCMR technique to be 84% calculated by using Equation (2) in Section 2.1.

In Table 1, several magnetic resonant coupling techniques available in the literature are compared with this work. As can be seen in Table 1, WPT distance is correlated with the radii of the Tx and Rx coils. Longer WPT distance requires larger radii of the Tx and Rx coils. Since the WSN proposed in this work operates in a small chamber, the miniaturization of the Tx and Rx coils is essential. While the radii of the Tx and Rx coils proposed in this study are the smallest ones in Table 1, the WPT distance and efficiency of this work are superior or comparable to other techniques with respect to $\frac{\text{Distance}}{\text{Radius of coil}}$ ratio.

3.2 | Rectifier and energy harvester

The photographs of fabricated PCBs for the rectifier and the transmitter of the WSN with the energy harvester are shown in Figure 6A. The RF power waveform at the rectifier input and the waveform at the output of the rectifier are compared to each other in Figure 4A. Figure 4B shows the output voltages and currents of the rectifier with respect to the peak input voltage from 3.6 to 10.2 V at 90 MHz. It also shows the temperature (−20°C vs. +25°C) characteristics. As can be seen in Figure 4B, the output voltage and current of the rectifier is slightly increased at −20°C. The peak input voltage of 10.2 V to the rectifier is used to operate the rectifier and energy harvester. The current supplied to the energy harvester from the rectifier at 20°C is 0.9 mA as shown in Figure 4B. By the Equation (3) with the v_{peak} of 10.2 V and I_{out} of 0.9 mA, the $\eta_{RF\text{-}DC}$ is 69% at 20°C. With the I_{out} of 0.95 mA at −20°C, $\eta_{RF\text{-}DC}$ is 76%.

Figure 5A,B shows the temperature characteristics of charging and discharging the supercapacitor. As can be seen in Figure 5, the temperature characteristics of the supercapacitor is excellent for low-temperature applications. The charging characteristic, as shown in Figure 5A, at −20°C is similar to that at 25. Although the charging time is very long, it is only 8% longer when compared to theoretical value of 80.3 h. The time duration ($\Delta t = t - t_0$) for the charging process can be calculated by using Equation (4), where the C, I_{charge}, and $v(t_0)$ are 480 F, 0.95 mA, and 2.455 V, respectively. The charging time at 25°C is 11.5 h longer than that at −20°C. This might come from heating the supercapacitor during the charging process.

$$\Delta t = \frac{C(v(t) - v(t_0))}{I_{charge}} = \frac{C\Delta v}{I_{charge}} \quad (4)$$

The discharging characteristic, as shown in Figure 5B, is very linear even at −20°C. The supercapacitor was discharged by operating continuously the transmitter of the WSN shown in Figure 6. When the transmitter operating, the transmitter consumes around 24 mA, which is $I_{discharge}$ in Equation (5). The measured voltage drop of 0.997 V is also very close to the theoretical value of 1.04 V calculated by Equation (5), where the C, $I_{discharge}$, and Δt are 480 F, 24 mA, and 5.82 h, respectively.

$$\Delta v = \frac{I_{discharge}(t - t_0)}{C} = \frac{I_{discharge}\Delta t}{C} \quad (5)$$

Figure 5B shows that low-temperature does not affect too much the discharge performance of the supercapacitor. The temperature independent performance of the supercapacitor makes supercapacitors perfect solution for energy storage unit for low temperature applications.

3.3 | Wireless sensor network

The WSN powered by WPT for low-temperature application is implemented as shown in Figure 6. The transmitter of the WSN is set up in a chamber to collect and send information

TABLE 1 Comparison of different magnetic resonant coupling techniques

Shape of coil	Radii of coils	Frequency (MHz)	Distance (mm)	Efficiency (%)	Applications
Single-turn wire (No thickness given)	Tx and Rx 150 mm	13.56	180	80	No application presented[17]
Circular spiral coil (No thickness given)	Tx 6 × 126 mm Rx 29 mm	1	50	74	Charging a smart phone[18]
Square spiral coil (Thickness = 0.54 mm)	Tx and Rx 50 mm × 50 mm	13.8	10	79	Monitoring system for implanted device[19]
Twelve-layer PCB (Thickness = 2 mm)	Tx and Rx 32 mm	20	60	78.2	No application presented[20]
Three-turn wire (No thickness given)	Tx and Rx 100 mm	7.0	200	86.8	No application presented[21]
Two-layer PCB (Thickness = 1.5 mm)	Tx and Rx 28 mm	90	60	84	WSN for low-temperature application [This work]

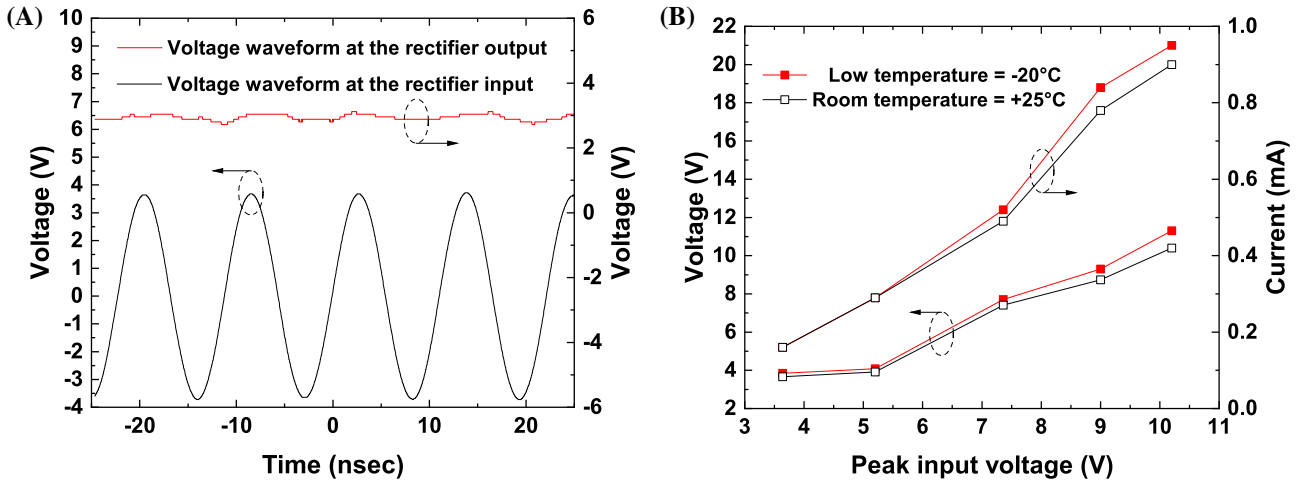

FIGURE 4 (A) Voltage waveforms at the input and output of the rectifier and (B) output voltages and currents of the rectifier with respect to the input voltage level

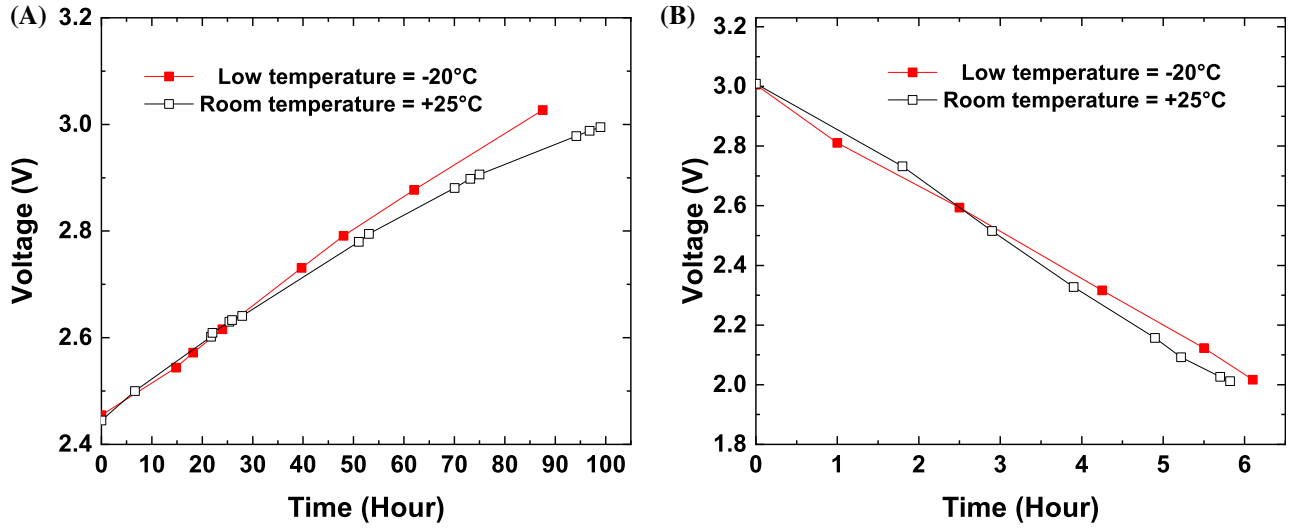

FIGURE 5 Temperature (−20°C vs. +25°C) characteristics of (A) charging and (B) discharging the supercapacitor

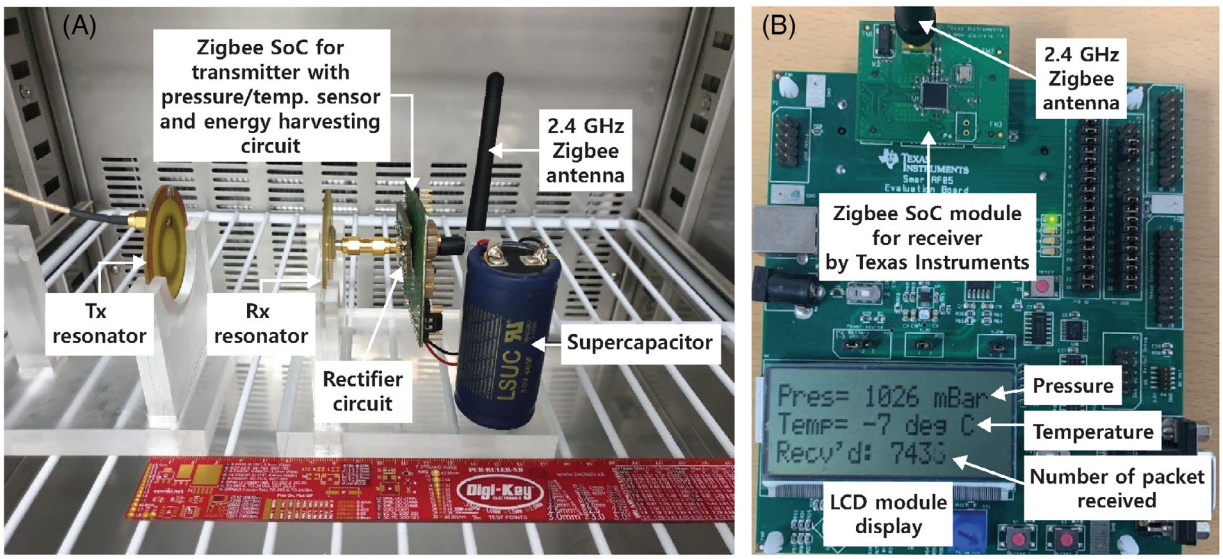

FIGURE 6 Photographs of the (A) transmitter powered by wireless power transfer system and (B) receiver of the wireless sensor network

of temperature and pressure in the chamber, as shown in Figure 6A. The receiver of the WSN, as shown in Figure 6B, is located outside the chamber.

Based on the charging and discharging characteristics presented in Section 3.2, one may establish an operating scenario for the WSN as follows. The packet sent from the transmitter has 24 bytes. The data rate of the WSN is set to be 250 kbps in this work. Therefore, it takes 0.758 ms to send the packet from the transmitter to receiver. The transmitter consumes maximum 2.6 μA in its sleep mode and takes 0.6 ms to transit from sleep mode to transmitting mode.[22]

Let us assume that the transmitter is in transmitting mode for 2 ms including sending a packet and transition from transmitting to sleep mode and it transmits environmental parameters 60 times per 1 h to the receiver. Then, it consumes 2.9 mA per an hour in the transmitting mode and in the rest of an hour, it consumes 9.4 mA in the sleep mode. For a day, the voltage drops 0.62 mV due to the operation of the WSN in this operating scenario. It takes only 331 s to charge the supercapacitor of 480 F with the charging current of 0.9 mA for the voltage drop of 0.62 mV. The supercapacitor can be charged seven times for 50 s during each sleep mode at the end of the day. As long as the circuit parts of the WSN operate properly, this WSN powered by WPT technique can operate without battery exchange process.

4 | CONCLUSIONS

We have demonstrated a self-sustainable WSN for low-temperature application. The WPT efficiency was 84% with the distance of 60 mm between transmitting and receiving resonators. The power conversion efficiency of the RF power rectifier is 69 and 76% at 25 and –20°C, respectively. To the rectifier, an energy harvester is added with a supercapacitor as an energy storage unit. The supercapacitor showed an excellent linearity in charging and discharging characteristics even at −20°C.

In an operating scenario, it was shown that the WSN can operate without battery exchange process. In this scenario, the WSN can collect environmental parameters such as temperature and pressure in a low temperature chamber every 1 min in a day. This design can be an excellent application of IoT used for monitoring the environment of a chamber where the pressure and temperature should be delicately controlled such as freeze dryers in pharmaceutical manufacturing industry.

ACKNOWLEDGMENT

This article was supported by Wonkwang University in 2020.

ENDNOTE

*High Frequency Structure Simulator, ANSYS, Inc., 2016.

DATA AVAILABILITY STATEMENT

The data that support the findings of this study are available from the corresponding author upon reasonable request.

ORCID


Young Seek Cho https://orcid.org/0000-0002-8011-0087

REFERENCES

[1] Lin J, Yu W, Zhang N, Yang X, Zhang H, Zhao W. A survey on internet of things: architecture, enabling technologies, security and privacy, and applications. *IEEE Internet Things J*. 2017;4(5):1125-1142. doi:10.1109/JIOT.2017.2683200

[2] Bagchi S, Abdelzaher TF, Govindan R, et al. New Frontiers in IoT: networking, systems, reliability, and security challenges. *IEEE Internet Things J*. 2020;7(12):11330-11346. doi:10.1109/JIOT.2020.3007690

[3] Sudevalayam S, Kulkarni P. Energy harvesting sensor nodes: survey and implications. *IEEE Commun Surveys Tutorials*. 2011;13(3):443-461. doi:10.1109/SURV.2011.060710.00094

[4] Kurs A, Karalis A, Moffatt R, Joannopoulos JD, Fisher P, Soljačić M. Wireless power transfer via strongly coupled magnetic resonances. *Science*. 2007;317(5834):83-86. doi:10.1126/science.1143254

[5] Hui SYR, Zhong W, Lee CK. A critical review of recent Progress in mid-range wireless power transfer. *IEEE Trans Power Electron*. 2014;29(9):4500-4511. doi:10.1109/TPEL.2013.2249670

[6] Shadid R, Noghanian S, Nejadpak A. A literature survey of wireless power transfer. *IEEE Int Conf Electro Inf Technol*. 2016;2016:782-787. doi:10.1109/EIT.2016.7535339

[7] Hu H, Bao K, Gibson J, Georgakopoulos SV. Printable and conformal strongly coupled magnetic resonant systems for wireless powering. *IEEE Annual Conf Wirel Microwave Technol*. 2014;2014:1-4. doi:10.1109/WAMICON.2014.6857762

[8] Fissore D, Pisano R, Barresi AA. On the use of temperature measurement to monitor a freeze-drying process for pharmaceuticals. 2017 IEEE International Instrumentation and Measurement Technology Conference (I2MTC); 2017:1-6. doi: 10.1109/12MTC.2017.7969890

[9] Grassini S, Fulginiti D, Pisano R, Oddone I, Parvis M. Real-time temperature monitoring in pharmaceutical freeze-drying. 2014 IEEE International Symposium on Medical Measurements and Applications (MeMeA); 2014:1-5. doi: 10.1109/MeMeA.2014.6860051

[10] Corbellini S, Parvis M, Vallan A. In-process temperature mapping system for industrial freeze dryers. *IEEE Trans Instrum Meas*. 2010;59(5):1134-1140. doi:10.1109/TIM.2010.2040909

[11] Cho YS, Kwon J, Choi S. Design and implementation of wireless sensor network for freeze dryer. *J Inf Commun Convergence Eng*. 2015;13(1):21-26.

[12] Ein-Eli Y, Thomas SR, Chadha R, Blakley TJ, Koch VR. Li-ion battery electrolyte formulated for low-temperature applications. *J Electrochem Soc*. 1997;144(3):823-829. doi:10.1149/1.1837495

[13] Smart MC, Ratnakumar BV, Surampudi S. Electrolytes for low-temperature lithium batteries based on ternary mixtures of aliphatic carbonates. *J Electrochem Soc*. 1999;146(2):486-492. doi:10.1149/1.1391633

[14] Huang CK, Sakamoto JS, Wolfenstine J, Surampudi S. The limits of low-temperature performance of Li-ion cells. *J Electrochem Soc*. 2000;147(8):2893. doi:10.1149/1.1393622

[15] Palazzi V, Del Prete M, Fantuzzi M. Scavenging for energy: a rectenna design for wireless energy harvesting in UHF Mobile telephony bands. *IEEE Microwave Mag*. 2017;18(1):91-99. doi:10.1109/MMM.2016.2616189

[16] Texas Instruments Incoporated. CC2530 Software Examples User's Guide; 2009. https://www.ti.com/lit/ug/swru214a/swru214a.pdf?ts=1638453113216

[17] Imura T, Hori Y. Maximizing air gap and efficiency of magnetic resonant coupling for wireless power transfer using equivalent circuit and Neumann formula. *IEEE Trans Industr Electron*. 2011;58(10):4746-4752. doi:10.1109/TIE.2011.2112317

[18] Jadidian J, Katabi D. *Magnetic MIMO: how to Charge your Phone in your Pocket*. ACM; 2014.

[19] Xu G, Yang X, Yang Q, Zhao J, Li Y. Design on magnetic coupling resonance wireless energy transmission and monitoring system for implanted devices. *IEEE Trans Appl Superconduct*. 2016;26(4):1-4. doi:10.1109/TASC.2016.6252491

[20] Bao K, Zekios CL, Georgakopoulos SV. Miniaturization of SCMR systems using multilayer resonators. *IEEE Access*. 2019;7:143445-143453. doi:10.1109/ACCESS.2019.2945319

[21] Shi L, Rasool N, Zhu H, Huang K, Yang Y. Design and experiment of a reconfigurable magnetic resonance coupling wireless power transmission system. *IEEE Microwave Wirel Compon Lett*. 2020;30(7):705-708. doi:10.1109/LMWC.2020.2997068

[22] Texas Instruments Incoporated. CC2530 datasheet (Rev. B); 2011. https://www.ti.com/lit/ds/symlink/cc2530.pdf?ts=1638471024728

How to cite this article: Cho YS, Choi K, Kwon J. Self-sustainable wireless sensor network for low-temperature application. *Microw Opt Technol Lett*. 2022;64:305–311. https://doi.org/10.1002/mop.33114